ELSEVIER

Marine Geology 217 (2005) 323–338

MARINE GEOLOGY
INTERNATIONAL JOURNAL OF MARINE GEOLOGY, GEOCHEMISTRY AND GEOPHYSICS

www.elsevier.com/locate/margeo

Biological overprint of the geological carbon cycle

Miriam E. Katz[a,*], James D. Wright[a], Kenneth G. Miller[a], Benjamin S. Cramer[b], Katja Fennel[c], Paul G. Falkowski[a,c]

[a]*Department of Geological Sciences, Rutgers University, 610 Taylor Road, Piscataway, NJ 08854, United States*
[b]*Institute of Geology and Paleontology, Tohoku University, Aoba, Aramaki, Sendai 980-8578, Japan*
[c]*Institute of Marine and Coastal Sciences, Rutgers University, 71 Dudley Road, New Brunswick, NJ 08901-8521, United States*

Received 21 May 2004; received in revised form 11 August 2004; accepted 2 March 2005

Abstract

The oxidation of Earth's atmosphere is coupled to the net sequestration of organic matter, which is related to the relative fractions of organic carbon (f_{org}) and carbonate (f_{carb}) buried in marine sediments. These fractions can be inferred from carbon isotope data. We present bulk sediment $\delta^{13}C$ records of carbonate ($\delta^{13}C_{carb}$) and organic carbon ($\delta^{13}C_{org}$) with a compilation of evolutionary trajectories of major eucaryotic phytoplankton for the past 205 million years. Our analysis indicates that changes in phytoplankton community structure, coupled with the opening of the Atlantic Ocean basin and global sea-level rise, increased the efficiency of organic carbon burial beginning in the Early Jurassic; in turn, this organic carbon burial increased the oxidation state of Earth's surface while drawing down atmospheric CO_2 levels (assuming no substantial negative feedbacks). The net oxidation and CO_2 drawdown appear to be related to the opening phase of the current Wilson cycle, where the newly formed passive plate margins store organic matter for hundreds of millions of years. This process should reverse during the closing phase of the Wilson cycle, when the continents reassemble and the Atlantic Ocean basin closes. The associated oxidation and storage of organic matter have contributed to the long-term depletion of CO_2, which was a key factor that selected C_4 photosynthetic pathways in marine and terrestrial ecosystems in the latter part of the Cenozoic; these pathways increasingly influenced $\delta^{13}C_{org}$, and ultimately contributed to the reversal of the long-term trend in $\delta^{13}C_{carb}$.

Keywords: carbon isotopes; organic carbon burial; oxidation state; Wilson cycle; phytoplankton

1. Introduction

The $\delta^{13}C$ signature of the ocean's mobile carbon reservoir is controlled by the $\delta^{13}C$ signatures and fluxes of carbon sources and sinks on timescales longer than the residence time of carbon in the oceans (~180

* Corresponding author. Tel.: +1 732 445 3445; fax: +1 732 445 3374.
E-mail address: mimikatz@rci.rutgers.edu (M.E. Katz).

0025-3227/$ - see front matter © 2005 Elsevier B.V. All rights reserved.
doi:10.1016/j.margeo.2004.08.005

kyr). The relationship between the sources (input) and sinks (output) of the geological carbon cycle is typically quantified using the standard equation that provides the backbone of carbon isotope models (e.g., Berner and Kothavala, 2001; Kump and Arthur, 1999):

$$f_w * \delta^{13}C_w + f_v * \delta^{13}C_v = f_{carb} * \delta^{13}C_{carb} + f_{org} * \delta^{13}C_{org} \quad (1)$$

where f=fraction, w=weathering, v=volcanic/hydrothermal, carb=carbonate, and org=organic carbon. Carbon is supplied to the ocean through outgassing from hydrothermal/volcanic activity and from erosion of continental rocks, while carbon is removed from the ocean through deposition of marine sediments. Over time, these sediments integrate large kinetic fractionations from photosynthetic reduction of CO_2 to organic matter with small thermodynamic fractionations from ion exchange reactions in carbonate precipitation. The relative fractions of carbonate and organic carbon buried in marine sediments are inferred from $\delta^{13}C$ records of carbonates and organic matter in sedimentary rocks (Hayes et al., 1999; Kump and Arthur, 1999). Changes in marine $\delta^{13}C_{carb}$ and $\delta^{13}C_{org}$ through time serve as archives of changes in carbon sources and sinks (for detailed summaries of the carbon cycle, see Hayes et al., 1999; Kump and Arthur, 1999).

In this study, we document and discuss long-term trends (tens to hundreds of million years) in $\delta^{13}C_{carb}$ and $\delta^{13}C_{org}$ records for the Jurassic–Cenozoic using both new and published data. We interpret the long-term trends based on GEOCARB III (Berner and Kothavala, 2001) model simulations that use these $\delta^{13}C_{carb}$ and $\delta^{13}C_{org}$ data, with additional information from comparisons with phytoplankton diversity records and geological proxies. Our goal is to investigate the geological and biological processes that interacted through time to produce these records of the global carbon cycle. A series of sensitivity tests based on Eq. (1) allows us to place constraints on potential variations in the carbon sources and sinks. Each of these sensitivity tests is designed to predict the maximum response to changing a single variable, and therefore does not take into account potential feedbacks through time that may have muted this response.

2. Methods

2.1. Site and sample selection

We measured $\delta^{13}C_{carb}$ on bulk sediment samples from Jurassic and Cretaceous sections (Figs. 1 and 2; Appendix A, web-archived at http://mychronos.chronos.org/~miriamkatz/20040728/). Bulk sediment samples were analyzed because they best characterize the inorganic carbon outflow from the ocean/atmosphere/biosphere, and provide the average $\delta^{13}C$ of the total carbonate produced and preserved in the marine system (Shackleton, 1987). This is the signal that is needed for the purposes of this paper; therefore, we use bulk sediment isotope records as a proxy for the average $\delta^{13}C$ of the inorganic output, allowing us to monitor long-term changes in the global carbon cycle through time (e.g., Shackleton, 1987). Although the mobile carbon reservoir in the deep ocean is substantially larger ($36\,700\times10^{15}$ g today) than the carbon reservoirs in the surface ocean and atmosphere (670×10^{15} g and 720×10^{15} g, respectively) (e.g., (Falkowski and Raven, 1997), relatively little sedimentary carbonate is produced in deepwaters. Therefore, a $\delta^{13}C$ record generated from deepwater benthic foraminifera does not provide a record of the average $\delta^{13}C$ of the total sedimentary carbonate preserved in the marine system. Rather, $\delta^{13}C$ analyses of benthic foraminifera record dissolved inorganic carbon (DIC) in deepwaters, and can be used to reconstruct deepwater circulation changes through time (e.g., Miller et al., 1987; Zachos et al., 2001); such a reconstruction is not the goal of this paper. A productivity signal can be extracted from benthic foraminiferal $\delta^{13}C$ only by comparing it with planktonic foraminiferal $\delta^{13}C$ from phosphate-free surface waters. Even then, it is only a proxy for the carbon to phosphorous ratio (C/P) (Broecker and Peng, 1982), which is proportional to productivity only as a function of stability/mixing. This would be impossible to do for the Jurassic–Cenozoic because planktonic foraminifera did not evolve until the Cretaceous and there is a lack of well-enough preserved foraminifera for a continuous Jurassic–Cretaceous isotope record.

Similarly, we do not use $\delta^{13}C_{carb}$ records generated from specific organisms (e.g., belemnites, oysters, and foraminifera), which reflect the different environments where each of those organisms lived (e.g.,

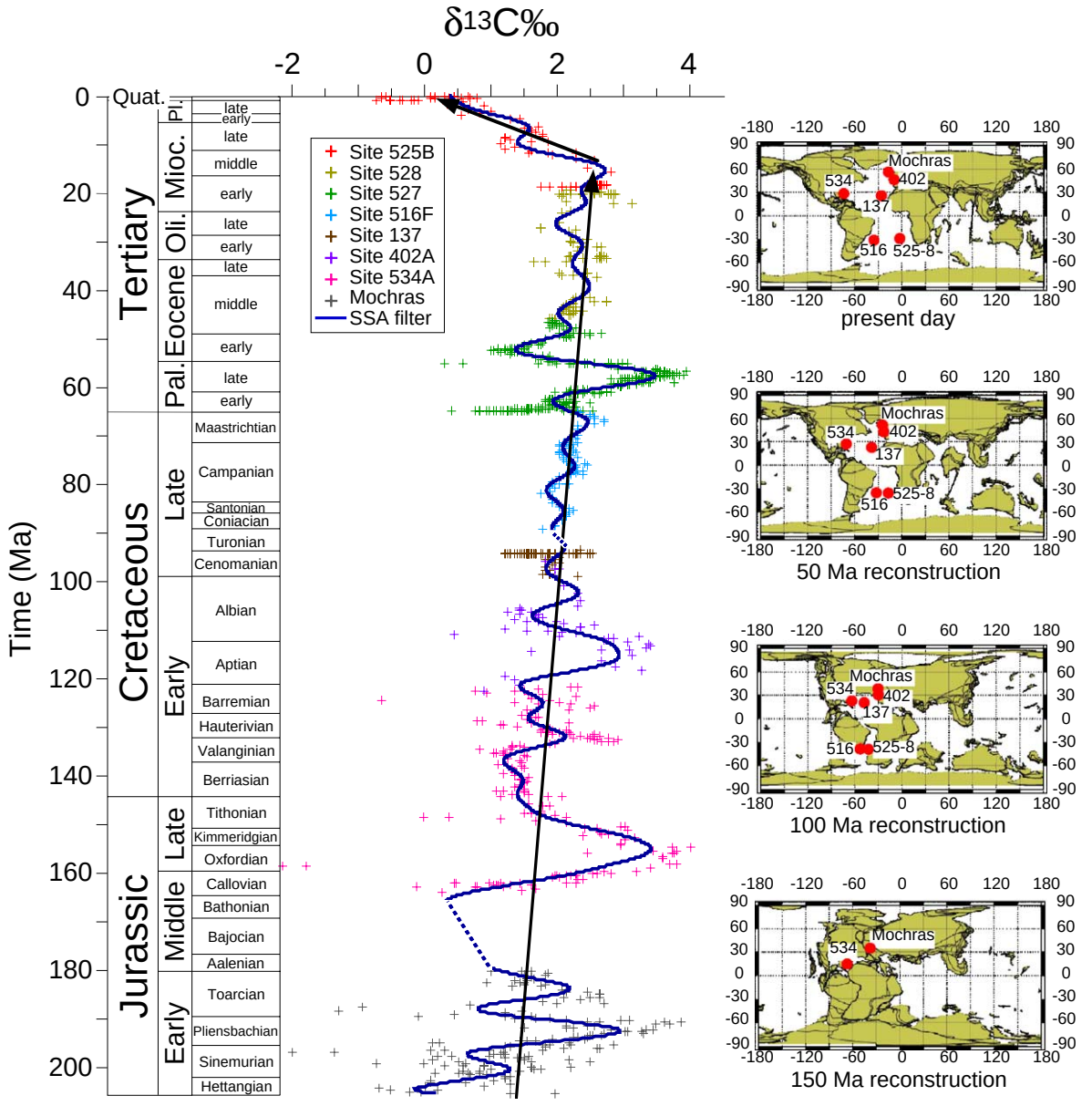

Fig. 1. Composite bulk sediment $\delta^{13}C$ record for the Jurassic through the Cenozoic (see Methods for site selection criteria). Mesozoic $\delta^{13}C$ data (this study) and Cenozoic $\delta^{13}C$ data (Shackleton and Hall, 1984) are primarily from open ocean Atlantic Deep Sea Drilling Project (DSDP) boreholes (see Methods). Data (Appendix A) are web-archived (http://www.mychronos.chronos.org/~miriamkatz/20040728/). Site locations are shown in a series of paleogeographic reconstructions at 50 myr intervals (http://www.odsn.de/odsn/index.html). We use least squares regression (95% confidence interval) to determine the long-term trends in $\delta^{13}C_{carb}$, where x=age and $y=\delta^{13}C_{carb}$: (1) $\Delta\delta^{13}C_{carb}=-2.52‰$ for 0–15 Ma: $y=(0.168\pm0.024)x+(0.049\pm0.17)$, $R=0.89$; (2) $\Delta\delta^{13}C_{carb}=1.1‰$ for 16–205 Ma: $y=(-0.006\pm0.001)x+(2.64\pm0.12)$, $R=0.38$. We note that including the Lower Jurassic section (Mochras borehole data) in the linear regression produces a lower rate of increase in $\delta^{13}C_{carb}$, which yields a more conservative estimate of the magnitude of the long-term increase. We use a singular spectrum analysis to highlight the long-term $\delta^{13}C_{carb}$ variations (see Methods).

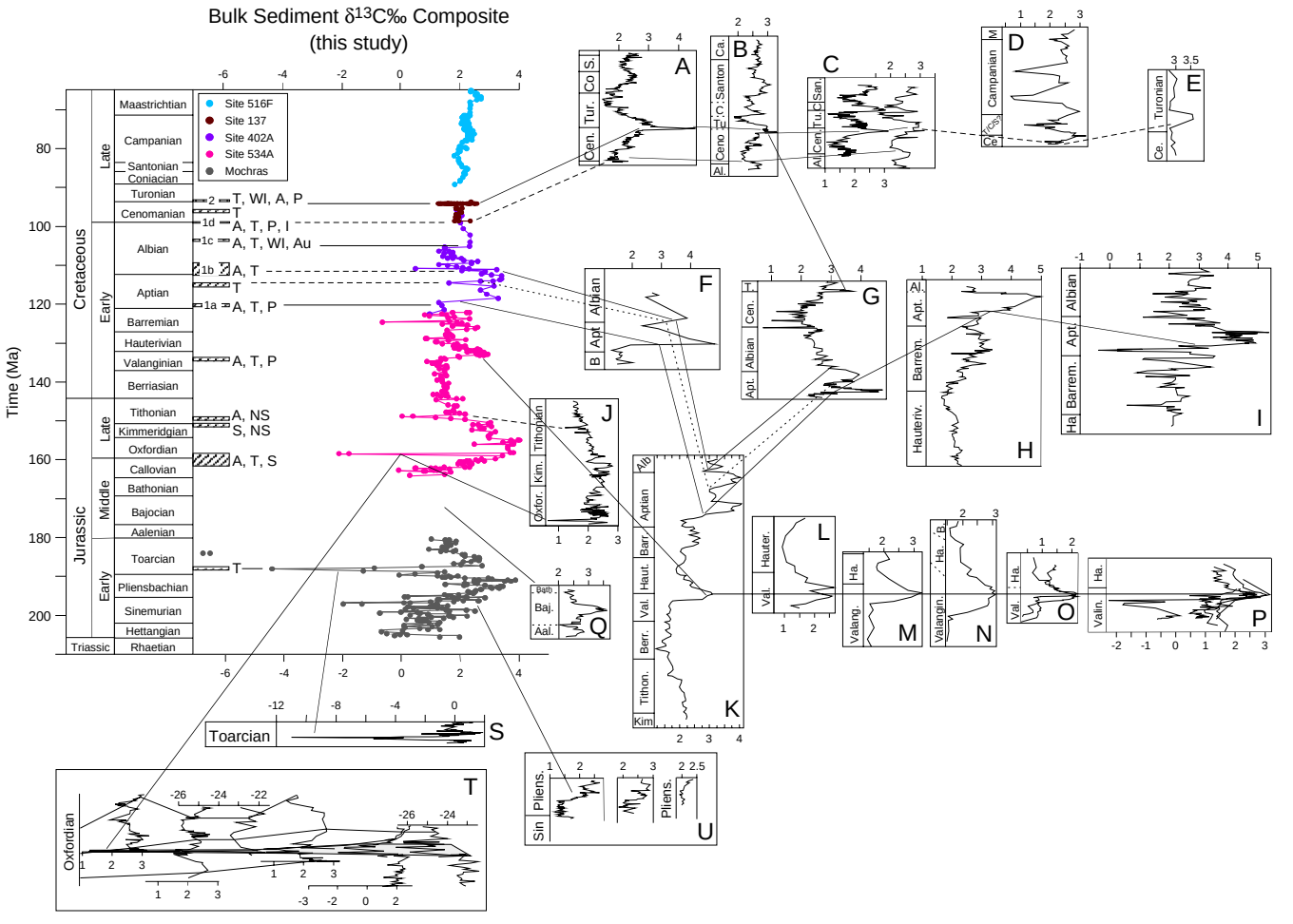

Fig. 2. Comparisons of the new Mesozoic $\delta^{13}C$ data with published bulk sediment $\delta^{13}C$ records: (A) Jenkyns et al. (1994); (B) Jenkyns et al. (1994); (C) Stoll and Schrag (2000); (D) Jenkyns et al. (1995); (E) Indian Ocean ODP Site 762C (Katz and Wright, unpublished data); (F) Atlantic Ocean ODP Site 641C (Katz and Wright, unpublished data); (G) Erbacher and Thurow (1997); (H) Erba et al. (1999), Menagatti et al. (1998); (I) Jenkyns et al. (1995); (J) Padden et al. (2002); (K) Weissert et al. (1998); (L) Hennig et al. (1999), van de Schootbrugge et al. (2000); (M) Channell et al. (1993); (N) Lini (1994); (O) Follmi et al. (1994); (P) Adatte et al. (2001); (Q) Bartolini et al. (1999); (R) Rohl et al. (2001); (S) Padden et al. (2001); (T) Morettini et al. (2002). Episodes and geographic distribution of elevated organic carbon deposition are indicated by slashed boxes next to the chronostratigraphic column (as summarized in Arthur et al., 1984; Leckie et al., 2002; Weissert et al., 1998). A=Atlantic, P=Pacific, T=Tethys, Au=Australia, NS=North Sea, WI=Western Interior of North America; S=Siberia; OAEs are labeled (1a), (1b), (1c), (1d) and, (2).

nearshore surface ocean vs. deep ocean bottom water) rather than the average $\delta^{13}C_{carb}$ output from the system. Furthermore, the $\delta^{13}C$ values can be complicated by the vital effects of specific organisms.

We rely on open ocean Atlantic Deep Sea Drilling Project (DSDP) boreholes (Fig. 1) with well-documented magnetobiostratigraphies that provide excellent age control and minimize the risk of undetected unconformities (Appendix B, web-archived at http://mychronos.chronos.org/~miriamkatz/20040728/). Even our oldest DSDP location (Site 534) was ~2500 m deep in the Middle Jurassic (Sheridan et al., 1983). Using open ocean locations circumvents problems that may be encountered in analyzing epicontinental sections, including unconformities associated with sea-level changes and local overprint of geochemical signals (e.g., Smith et al., 2001). However, it was necessary to use an epicontinental section for the older record because there is little to no pre-Middle Jurassic ocean floor left. We chose the Mochras borehole (Wales) because it spans the entire Lower Jurassic at a single location and its lithology and biostratigraphy are well documented (Ivimey-Cook, 1971; Woodland, 1971). There are several data gaps in our record: 1) no Atlantic DSDP/ODP borehole contains conclusive in situ Turonian sediments; and 2) no Aalenian–Bathonian sections were available for analysis, nor were published bulk sediment $\delta^{13}C_{carb}$ records with firm age constraints available.

2.2. Age models

Age models for the isotope data were developed using magnetobiostratigraphy from published records (Appendix B, web-archived at http://www.mychronos.chronos.org/~miriamkatz/20040728/). Ages are calibrated to the time scales of Berggren et al. (1995; Cenozoic) and Gradstein et al. (1995; Mesozoic). Ages are assigned to data by interpolating between data and across time intervals that are substantially longer than the sample spacing, with the potential to introduce a margin of error when multiple datasets are combined within a single time interval. We minimize this potential error by using a composite record (individual records stacked one on top of the other) rather than a compilation (overlay of multiple records) to insure that the chronological integrity of our records is intact.

2.3. Stable isotope analyses

Stable isotope analyses on Mesozoic samples were performed in the Stable Isotope Laboratory at Rutgers University using a multi-prep peripheral device and analyzed on an Optima mass spectrometer. Samples were reacted in 100% phosphoric acid at 90 °C for 13 min. Values are reported vs. V-PDB through the analysis of an internal standard calibrated with NBS-19 (1.95‰ for $\delta^{13}C$) as reported by Coplen et al. (1983) and Coplen (1995).

2.4. Statistical analysis

$\delta^{13}C$ data were linearly interpolated (100 kyr sampling interval) and analyzed using the SSA-MTM Toolkit from http://www.atmos.ucla.edu/tcd/ssa/ (Ghil et al., 2002). Singular Spectrum Analysis (SSA) was performed using a 205 point (~20 myr) window with the Broomhead and King method for constructing the covariance matrix; the six highest variance components were added together to reconstruct the long-term $\delta^{13}C$ variations shown by the curve in Fig. 1.

In addition, we use least squares regression (95% confidence interval) to determine the long-term trends in $\delta^{13}C_{carb}$ and $\delta^{13}C_{org}$. We note that including the Lower Jurassic section (Mochras borehole data) in the linear regression produces a lower rate of increase in $\delta^{13}C_{carb}$, which yields a more conservative estimate of the magnitude of the long-term change.

3. Results and discussion

3.1. Carbon isotope records

We constructed a composite bulk sediment $\delta^{13}C_{carb}$ record using new Mesozoic data (this study) and published Cenozoic data (Shackleton and Hall, 1984) (Fig. 1). Comparisons of the new Mesozoic data with shorter-duration published bulk sediment $\delta^{13}C$ records establish that the composite curve records global $\delta^{13}C$ changes in the Cretaceous (Fig. 2). Our Jurassic record is derived from the Tethys and the small, nascent Atlantic, with no published bulk sediment $\delta^{13}C$ records from open ocean settings for comparison. Therefore, we cannot conclusively establish that our Jurassic record reflects a global signal;

nonetheless, we note that our data trends are consistent with the compilation of Veizer et al. (1999). Episodes and geographic distribution of elevated organic carbon deposition are indicated in blue on the chronostratigraphic column (as summarized in Arthur et al., 1984; Leckie et al., 2002; Weissert et al., 1998).

Most of the shorter-term events recorded in our data have been well documented in other publications, such as: 1) extended periods (~5–10 myr) of elevated $\delta^{13}C$ values (e.g., Early Jurassic, Late Jurassic, Aptian–early Albian, Paleocene–early Eocene); 2) rapid, transient $\delta^{13}C$ decreases (Toarcian, Oxfordian, Tithonian, Albian, Aptian, Cenomanian/Turonian, Cretaceous/Tertiary boundary, and Paleocene/Eocene boundary); and 3) short-lived ($\lesssim$1 myr) $\delta^{13}C$ increases associated with the well-documented oceanic anoxic events. Perturbations in the carbon cycle lasting $\lesssim$10 myr typically are attributed to changes in the biological processes that are responsible for export production and/or the geological processes that are responsible for sediment preservation (Miller and Fairbanks, 1985; Scholle and Arthur, 1980; Vincent and Berger, 1985), rapid (<100 000 yr) exchanges between carbon reservoirs (Dickens et al., 1995; Kurtz et al., 2003), or accretion of extraterrestrial carbon (Kent et al., 2003; Wilde and Quinby-Hunt, 1997). Because these short-duration global $\delta^{13}C$ events are recorded in our bulk sediment $\delta^{13}C_{carb}$ record, we can infer that the primary isotopic signal is preserved with little to no diagenetic overprint.

Our composite bulk sediment $\delta^{13}C_{carb}$ record reveals a 190 myr long increase of ~1.1‰ from the Jurassic through the mid-Miocene and a subsequent ~2.5‰ decrease (Fig. 1; see figure caption for details of regression). We focus on these two trends in this paper, rather than the well-documented, shorter $\delta^{13}C$ events that punctuate these trends, and which have been the topic of many previous publications (see Methods). The ~1.1‰ increase in our composite bulk sediment $\delta^{13}C_{carb}$ record (Fig. 1) can be supported by combining Figs. 2 and 3 from Hayes et al. (1999); when spliced together, the resulting $\delta^{13}C_{carb}$ record shows a long-term increase of ~1‰ (~1.5‰ to ~2.5‰) from 200 to 20 Ma that was not identified by Hayes et al. (1999) and has not been reported previously. The long-term trends in the bulk sediment $\delta^{13}C_{carb}$ record from sites with different burial depth histories also argue against diagenetic overprint because diagenesis would not produce a systematic differential offset through time.

3.2. Jurassic to mid-Miocene 1.1‰ $\delta^{13}C_{carb}$ increase

Comparison of carbonate and organic carbon isotope records provides the best means to monitor changes in the geological carbon cycle (Kump and Arthur, 1999) (Fig. 3). The $\delta^{13}C_{org}$ record shown here was adapted from Hayes et al. (1999), who compiled published and unpublished $\delta^{13}C_{org}$ data for marine organic matter, modified the data based on several criteria (see Hayes et al., 1999 for details of their data manipulation), and plotted a smoothed curve (the record shown here uses their data rather than their smoothed curve). The simultaneous increases in $\delta^{13}C_{carb}$ (this study) and $\delta^{13}C_{org}$ (Hayes et al., 1999) highlight a long-term increase in $\delta^{13}C$ of the mobile carbon reservoir (Fig. 3; see figure caption for details of statistics). Two processes could have driven this long-term $\delta^{13}C$ increase: (1) an increase in the $\delta^{13}C$ of input carbon ($\delta^{13}C_{input}$); and/or (2) an increase in the fraction of organic carbon buried (f_{org}).

3.2.1. Model results

To investigate the two processes that could have contributed to the long-term $\delta^{13}C$ increase (changes in $\delta^{13}C_{input}$ and f_{org}; see previous section), we ran model simulations based on a derivation of Eq. (1):

$$f_{org} = \left[\left(\delta^{13}C_{input}\right) - \left(f_{carb} * \delta^{13}C_{carb}\right)\right] / \delta^{13}C_{org} \qquad (2)$$

Two model runs (Fig. 4) that use the $\delta^{13}C_{carb}$ (this study) and $\delta^{13}C_{org}$ (Hayes et al., 1999) datasets and allow the model to calculate the burial fractions of carbonate vs. organic carbon are shown. In the first model run, $\delta^{13}C_{input}$ was allowed to vary according to GEOCARB III (Berner and Kothavala, 2001) parameters that are based on various feedbacks and variables, such as the influence of land plants, erosion rates, paleogeography, and global continental water discharge (see Berner and Kothavala, 2001 for details of the model). In the second simulation, $\delta^{13}C_{input}$ was held constant at −5‰, based on the assumption that carbonate and organic carbon weathering from continents averages out to the mantle carbon value over long time periods (e.g., Kump and Arthur, 1999).

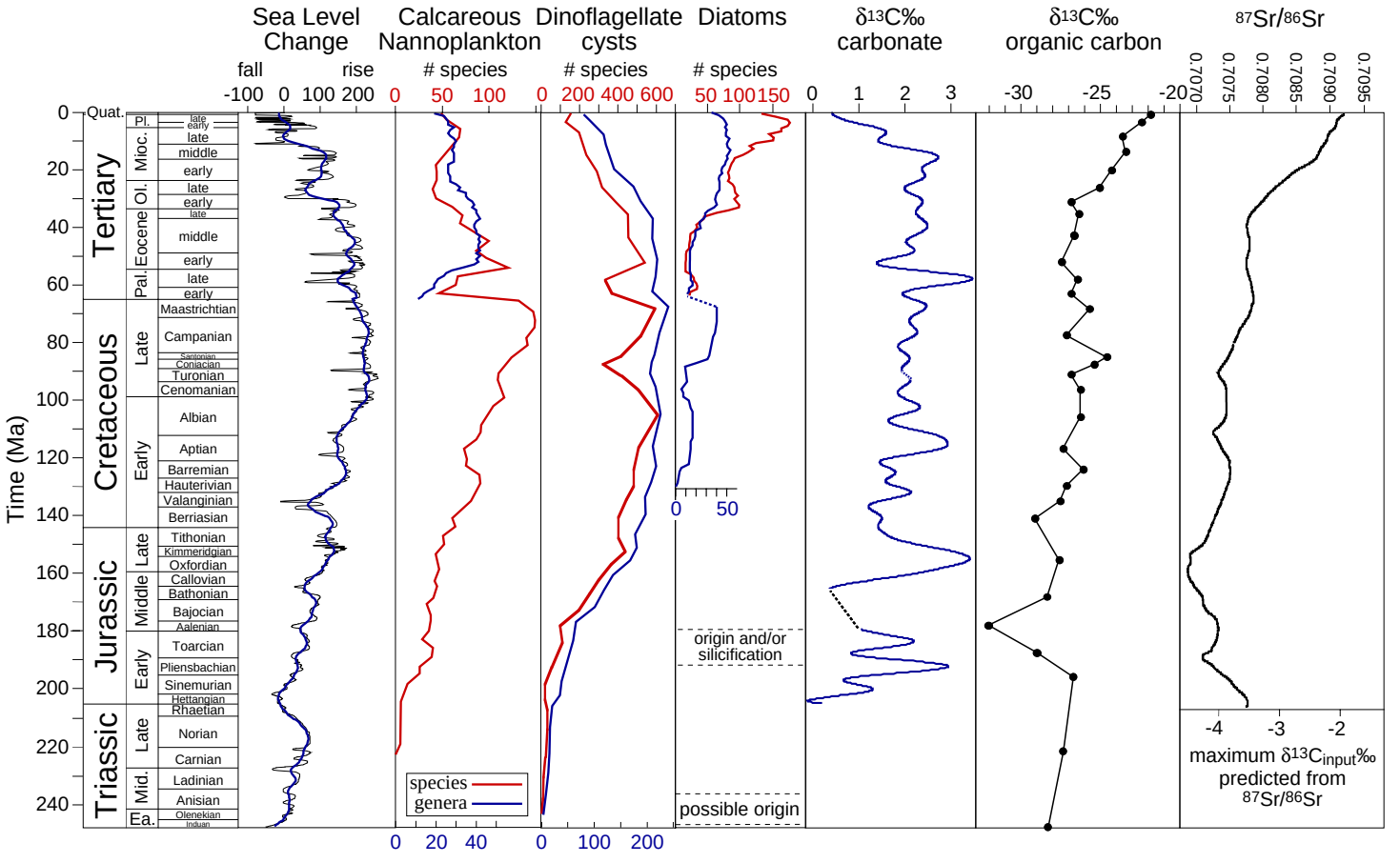

Fig. 3. Comparison of eucaryotic phytoplankton diversity curves with sea-level change (Haq et al., 1987), $\delta^{13}C_{carb}$ (this study), $\delta^{13}C_{org}$ (Hayes et al., 1999, without their smoothed curve through the data; see Section 3.2), and strontium isotopes (Howarth and McArthur, 1997). Phytoplankton species diversities are from published studies (calcareous nannofossils, Bown et al., 2004; dinoflagellates, Stover et al., 1996; diatoms, Spencer-Cervato, 1999). Phytoplankton genus diversities were compiled for this study from publicly available databases (Cenozoic calcareous nannofossils and diatoms, Spencer-Cervato, 1999; dinoflagellates, MacRae, unpublished data; Mesozoic diatoms, Harwood and Nikolaev, 1995). All records are adjusted to a uniform time scale (Berggren et al., 1995; Gradstein et al., 1995). We use least squares regression (95% confidence interval) to determine the long-term trends in $\delta^{13}C_{org}$, where x=age and $y=\delta^{13}C_{org}$: (1) $\Delta\delta^{13}C_{org}$=4.4‰ for 0–31.1 Ma: $y=(-0.14\pm0.036)x+(-21.89\pm0.66)$, R=0.96; (2) $\Delta\delta^{13}C_{org}$=1.7‰ for 31.1–190 Ma: $y=(-0.011\pm0.0088)x+(-25.88\pm0.99)$, R=0.5 (outlier at 177.98 Ma was omitted from analysis). See Fig. 1 for $\delta^{13}C_{carb}$ regression. $\delta^{13}C_{input}$ is predicted from $^{87}Sr/^{86}Sr$ based on a simple two-source system that predicts the maximum increase in $\delta^{13}C_{input}$. The primary sources of strontium and carbon in the oceans are hydrothermal/volcanic ($^{87}Sr/^{86}Sr$=0.7064; $\delta^{13}C$=−5‰) and continental erosion (high $^{87}Sr/^{86}Sr$=0.711 and $\delta^{13}C$=0‰; we assume carbonate weathering to constrain the maximum possible increase in $\delta^{13}C_{input}$, and note that erosion of continental shales yields lower $\delta^{13}C_{input}$) (Hodell et al., 1989; Kump and Arthur, 1999). To constrain the maximum end-member predicted $\delta^{13}C_{input}$ increase, we use the maximum rate of $^{87}Sr/^{86}Sr$ increase prior to the Cenozoic inflection point (158.5–38.5 Ma; $^{87}Sr/^{86}Sr=(-0.0000065\pm0.0000001)age+(0.70810\pm.000007)$, R=0.90).

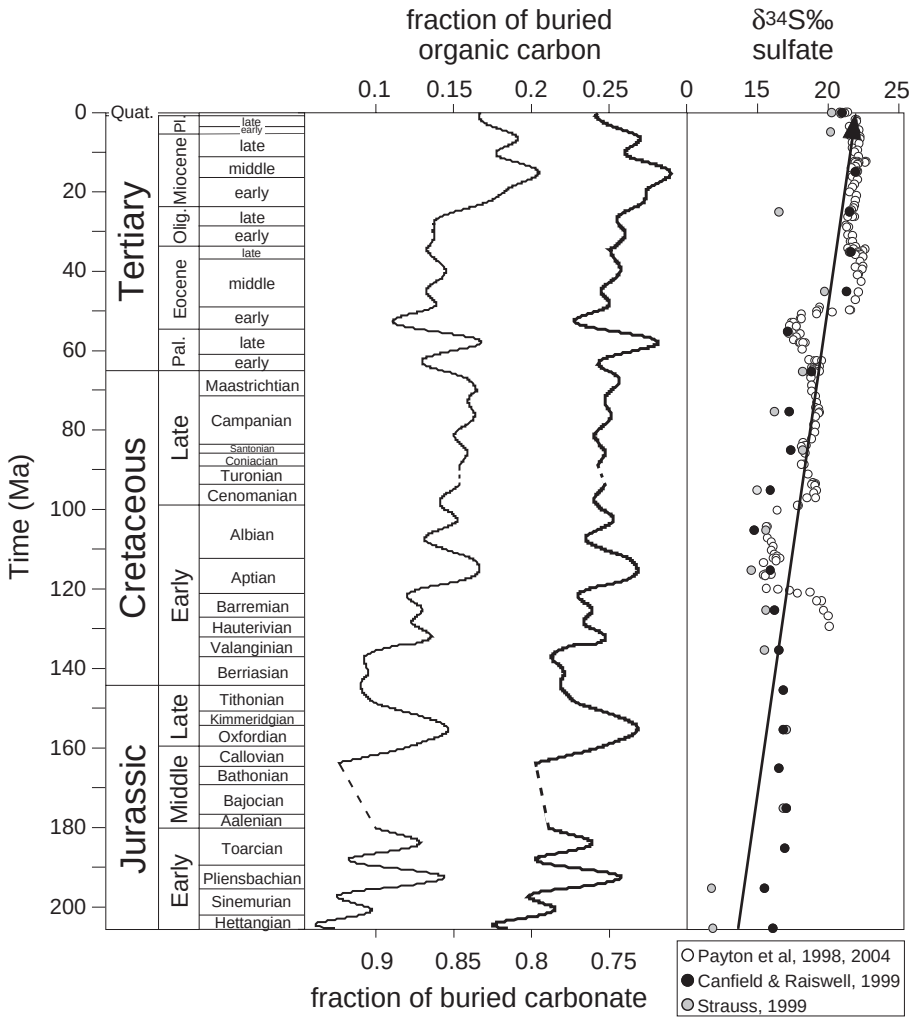

Fig. 4. Comparison of model simulations of f_{org} and f_{carb} (this study) and published sulfur isotopes. Two model simulations predict the burial fractions of carbonate and organic carbon using Eq. (2). Each simulation uses $\delta^{13}C_{carb}$ (this study) and $\delta^{13}C_{org}$ (Hayes et al., 1999). In the first simulation (thin line), $\delta^{13}C$ of input carbon ($\delta^{13}C_{input}$) is allowed to vary according to Berner and Kothavala (2001). In the second simulation (thick line), $\delta^{13}C_{input}$ is held constant at −5‰ (mantle carbon value) (e.g., Kump and Arthur, 1999). Increasing values of $\delta^{34}S$ in marine sulfate from the Jurassic to the present indicate that ^{32}S-enriched sediments were buried through biologically mediated sulfate reduction of organic matter, thus supporting the f_{org} increase. We note that Mesozoic $\delta^{34}S$ data are sparse. We use least squares regression (95% confidence interval) to determine the long-term trends in $\delta^{34}S$ (Canfield and Raiswell, 1999; Paytan et al., 1998, 2004; Strauss, 1999), where x=age and $y=\delta^{34}S$ of sulfate: $y=(-0.042\pm0.002)x+(22.04\pm0.15)$, $R=0.82$.

Both of these modeling efforts show that the increases in $\delta^{13}C_{carb}$ and $\delta^{13}C_{org}$ require an f_{org} increase of ~0.05–0.1, regardless of whether $\delta^{13}C_{input}$ varied (Berner and Kothavala, 2001) or was constant (Kump and Arthur, 1999) (Fig. 4). This requires greater burial efficiency (i.e., long-term sequestration) of organic matter in marine and/or terrestrial environments.

3.2.2. Phytoplankton evolution, carbon burial, and the Wilson cycle

The greater burial efficiency of marine organic matter that is indicated by our model simulations resulted from a combination of increases in export production and organic carbon preservation on the seafloor. In this section, we investigate changes in

marine primary producers (phytoplankton). We use taxonomic diversity as a proxy for phytoplankton evolution, although a spectrum of floral changes could also be used to address the adaptation of eucaryotic phytoplankton to changes in ocean conditions (e.g., structural innovations in phytoplankton or size trends through time).

The long-term increases in $\delta^{13}C_{carb}$ and $\delta^{13}C_{org}$ that began in the Mesozoic were accompanied by major evolutionary changes among the primary producers in the marine biosphere (Fig. 3). Three groups of eucaryotic marine phytoplankton (calcareous nannoplankton, dinoflagellates, and diatoms) began their evolutionary trajectories to ecological prominence as the supercontinent Pangea began to break apart in the Late Triassic–Early Jurassic (~200 myr ago), marking the opening phase of the current Wilson cycle (Wilson, 1966; Worsley et al., 1986) of continental break-up, dispersal, and reassembly. As Pangea fragmented and the Atlantic Ocean basin widened, the total length of coastline increased and sea level rose, flooding continental shelves and low-lying continental interiors. Nutrients that were previously locked up in the large continental interior of Pangea were transported to newly formed shallow seas and distributed over wider shelf areas and longer continental margins.

The diversity increases in the three groups of eucaryotic phytoplankton parallel the long-term sea-level increase that began in the Early Jurassic (Haq et al., 1987) (Fig. 3). Greater nutrient availability, coupled with expanded ecological niches and increased ecospace, appears to have selected for phytoplankton that lived along continental margins and contributed to their rapid radiation and evolution, a trend that prevailed as sea level continued to rise through the Mesozoic. The Cretaceous/Tertiary boundary bolide impact caused mass extinctions (Alvarez et al., 1980) that are recorded in the fossil records of the coccolithophores and, to a lesser extent, the diatoms and dinoflagellates (Fig. 3). The ensuing collapse of organic matter export and burial is recorded as a rapid decrease in $\delta^{13}C_{carb}$ (Fig. 1) (D'Hondt et al., 1998). Dinoflagellates and calcareous nannoplankton recovered to pre-extinction diversity levels by the earliest Eocene (~55 Ma), only to decline through the rest of the Cenozoic as long-term sea level began to fall in the mid-Paleogene. In contrast, diatom diversity increased as diversities in the other two groups decreased.

The radiation of large eucaryotic marine phytoplankton in the Mesozoic (Grantham and Wakefield, 1988; Moldowan and Jacobson, 2000) that efficiently exported organic matter contributed to an overall increase in export production through time (Bambach, 1993; Falkowski et al., 2003). Much of the export production is concentrated along continental margins today (Laws et al., 2000; Walsh, 1988), where up to 90% of organic carbon burial occurs (Hedges and Keil, 1995). In the same manner, substantial amounts of organic carbon were sequestered on the newly formed passive continental margins of the Atlantic and on flooded continental interiors (Arthur et al., 1984; Bralower, 1999; Claypool et al., 1977; Jenkyns and Clayton, 1997) as Pangea broke apart. Global sediment budgets indicate that an order of magnitude more sediment is deposited in ocean basins than is subducted (Rea and Ruff, 1996), and that the long-term marine sedimentary system can be at steady state only over a complete Wilson cycle (Mackenzie and Pigott, 1981; Rea and Ruff, 1996; Worsley et al., 1986); we note that sedimentary accretion on cratons has the potential to keep the system out of balance even over several Wilson cycles. The circum-Atlantic sediments have not yet been recycled through subduction or uplift and erosion, and effectively have become geological stores of organic matter. The net effect of the long-term storage of large amounts of isotopically light organic carbon has been to increase the $\delta^{13}C$ of the remaining inorganic carbon reservoir (Fig. 1).

3.2.3. Changes in f_{org} vs. $\delta^{13}C_{input}$

A series of simple sensitivity tests based on Eq. (1) helps to constrain the likelihood that changes in f_{org} and/or $\delta^{13}C_{input}$ contributed to the 1.1‰ increase in $\delta^{13}C_{carb}$. A ~20% increase in f_{org} from 205 Ma to ~30 Ma is required to account for the measured changes in $\delta^{13}C_{carb}$ and $\delta^{13}C_{org}$. Integrated over time (assuming a linear increase in f_{org}, constant carbon reservoir size, and 300 000 Gt/myr carbon burial flux; Berner and Kothavala, 2001), this increase requires that an additional ~1.1 million Gt ($=91\times10^{18}$ mol) of organic carbon was buried at the expense of inorganic carbon beyond the initial burial conditions at the beginning of the current Wilson cycle.

This organic matter could have been buried in marine and/or terrestrial environments. However, the partitioning of organic burial between the marine and terrestrial realms cannot be quantified. We estimate the order of magnitude for reasonable terrestrial organic carbon burial based on models of the Paleocene $\delta^{13}C_{carb}$ perturbation—an event proposed to be the result of excessive terrestrial organic carbon burial (Kurtz et al., 2003), 1.25×10^{18} mol of terrestrial organic carbon buried over 10 myr. If similar elevated rates were sustained from 205 Ma to ~30 Ma, it would result in the burial of 21.9×10^{18} mol of total terrestrial organic carbon. Although this is simply an upper limit estimate to provide an idea of the order of magnitude of potential terrestrial organic carbon burial, we note that it is at most only ~25–30% of the predicted excess carbon burial. Therefore, we conclude that marine carbon burial must have constituted most of the f_{org} increase.

Geologic evidence for high organic carbon burial in the circum-Atlantic region as Pangea broke apart in the Jurassic–Cretaceous (Arthur et al., 1984; Bralower, 1999; Claypool et al., 1977; Jenkyns and Clayton, 1997) supports the hypothesis that an increase in marine organic carbon burial contributed to the measured changes in $\delta^{13}C_{carb}$. Strong evidence for the associated drawdown of atmospheric CO_2 is provided by proxy records that show a long-term decline in atmospheric CO_2 levels over the same time period (see Royer et al., 2004 for review; proxy records include $\delta^{13}C$ data from paleosols and phytoplankton, stomatal distribution in leaves, $\delta^{11}B$ from planktonic foraminifera, and geochemical models). In addition, an integrated carbon–calcium–strontium model predicts that enhanced precipitation and erosion following the break-up of Pangea contributed to greater nutrient availability in the oceans, driving a productivity increase that resulted in greater marine organic carbon burial over the past 150 myr (Wallmann, 2001). Additional modeling predicts that elevated export production and organic carbon burial rates should enhance reducing conditions at the seafloor and facilitate release of phosphate from sediments; the resulting positive feedback generated by this nutrient recycling can further enhance export production (Wallmann, 2003). In this manner, expansion of the large-cell eucaryotes in the Mesozoic and organic carbon storage along the circum-Atlantic passive margins may have favored phosphorous availability and high rates of export production, facilitating the f_{org} increase predicted by our $\delta^{13}C$ records and model simulations. This scenario is supported by increasing values in marine sulfate $\delta^{34}S$ (Fig. 4) that indicate increases in pyrite burial, which is dependent on high levels of sedimentary organic matter.

Assuming that oxygenic photosynthesis was the ultimate source of this buried organic matter (whether of terrestrial or marine origin), mass balance requires that 3.0 million Gt of oxygen was produced over the 205 myr interval. In the absence of substantial negative feedbacks, the atmospheric inventory of O_2 would have at least tripled as a result. Greater O_2 production via organic carbon burial should drive greater O_2 production through pyrite burial (Berner et al., 2003). This is supported by the coeval increase in $\delta^{34}S$ (Fig. 4), which indicates that the sedimentary reservoir of reduced sulfur (=pyrite) increased, requiring a corresponding increase in oxidized species. Therefore, the coeval increases in f_{org} and $\delta^{34}S$ (Fig. 4) indicate that the oxidation state of Earth's surface reservoirs increased. Several modeling and sulfur isotope studies conclude that it is unlikely that atmospheric O_2 levels increased by as much as threefold (Berner et al., 2003; Hansen and Wallmann, 2003; Paytan et al., 1998; Strauss, 1999); if this is correct, then either some of the excess oxygen was consumed through oxidation of surface carbon and sulfur reservoirs (Hansen and Wallmann, 2003), or the $\delta^{13}C$ of the mobile carbon reservoir was controlled not only by excess burial of organic carbon, but also by an increase in $\delta^{13}C_{input}$.

A simple sensitivity test using Eq. (1) shows that to produce the measured $\delta^{13}C_{carb}$ and $\delta^{13}C_{org}$ trends without changing f_{org} requires that $\delta^{13}C_{input}$ increased by 1.76‰. To predict whether $\delta^{13}C_{input}$ could have increased as much as 1.76‰, we use a sensitivity test based on the $^{87}Sr/^{86}Sr$ record, given that both carbon and strontium are supplied to the oceans from the same sources (hydrothermal activity and continental weathering) (Fig. 3; see caption for details). We assume that riverine delivery of carbon to the oceans was dominated by carbonate erosion in order to constrain the maximum potential increase in $\delta^{13}C_{input}$ due to changes in continental weathering,

and note that erosion of continental shales would act to decrease the maximum predicted $\delta^{13}C_{input}$. Similarly, we use the maximum rate of $^{87}Sr/^{86}Sr$ increase (prior to the Himalayan/Tibetan uplift) to constrain the maximum end-member predicted $\delta^{13}C_{input}$ increase (Fig. 3; see figure caption for details). Results of this sensitivity analysis show that $\delta^{13}C_{input}$ could have increased by no more than 0.87‰; in reality, the increase was most likely less, based on the assumptions listed above. The maximum predicted increase is approximately half of the increase in $\delta^{13}C_{input}$ required to account for the measured $\delta^{13}C_{carb}$ and $\delta^{13}C_{org}$ changes if f_{org} were held constant. Therefore, it is likely that both f_{org} and $\delta^{13}C_{input}$ increased, in effect both supplying more ^{13}C to and extracting more ^{12}C from the mobile carbon reservoir to drive the observed 1.1‰ increase in $\delta^{13}C_{carb}$ during the opening phase of the current Wilson cycle.

Our results support the hypothesis that the Phanerozoic Wilson cycles drove the greenhouse–icehouse cycles. In this scenario, Fischer (1984) proposed that volcanic CO_2 outgassing during continental fragmentation created greenhouse climates, and that atmospheric CO_2 drawdown due to weathering processes eventually switched the planet to an icehouse mode. Our results indicate that there is a significant biological component that contributes to the climate switch. In this important additional biological loop, changes in phytoplankton community structure contributed to greater efficiency of organic carbon burial beginning in the Early Jurassic. The excess carbon burial that drove the net oxidation of Earth's surface reservoirs and atmospheric CO_2 drawdown during the opening phase of the current Wilson cycle ultimately contributed to the climate change from the greenhouse conditions of the Mesozoic to the icehouse conditions that characterize the latter half of the Cenozoic.

3.3. A 2.5‰ $\delta^{13}C_{carb}$ decrease since the mid-Miocene

$\delta^{13}C_{org}$ began to increase more rapidly at ~30 Ma, while the rate of increase in $\delta^{13}C_{carb}$ remained relatively constant until ~15 Ma (Fig. 3). These results indicate that f_{org} increased during this interval to the highest level of the past 205 Ma (Fig. 4), culminating in the "Monterey Carbon Excursion" in which large amounts of organic-rich, diatomaceous sediments were deposited in marginal basins (Vincent and Berger, 1985).

The $\delta^{13}C_{carb}$ trend reversed in the Neogene, with values that have decreased by ~2.5‰ since ~15 Ma (Fig. 1) (Shackleton and Hall, 1984), while $\delta^{13}C_{org}$ values continued to increase (Hayes et al., 1999) (Figs. 1 and 3). This requires a ^{12}C increase in the mobile carbon reservoir through more ^{12}C supply and/or less ^{12}C burial. $^{87}Sr/^{86}Sr$ and $^{187}Os/^{186}Os$ records indicate a shift in the Neogene to continental source rocks rich in organic carbon, which may have increased the supply of ^{12}C to the oceans even though continental weathering rates may have decreased (Derry and France-Lanord, 1996; Ravizza, 1993; Turekian and Pegram, 1997). If the total carbon flux (Berner, 1991) were constant, then an additional ~194 000 Gt of carbon from organic carbon weathering (at the expense of carbonate weathering) can account for the entire 2.5‰ $\delta^{13}C_{carb}$ decrease. Although erosion of organic-rich black shales may account for part of the 2.5‰ $\delta^{13}C_{carb}$ decrease, we present an alternative hypothesis based on a secular increase in $\delta^{13}C_{org}$ (Fig. 3).

Large phytoplankton cells tend to produce high $\delta^{13}C_{org}$ because they tend to have low growth rates and low rates of diffusive flux (Laws et al., 1997; Popp et al., 1998; Rau et al., 1997). Based on this concept, Hayes et al. (1999) proposed that a trend towards low CO_2 levels (Freeman and Hayes, 1992), rapid cell growth rates, and large cell volume relative to surface area began in the early Oligocene, and that these changes resulted in lower photosynthetic fractionation factors that contributed to the $\delta^{13}C_{org}$ increase. However, the median diatom cell size appears to have decreased through the Cenozoic (Finkel et al., in press), contradicting the hypothesis of Hayes et al. (1999) that a trend towards larger diatoms alone drove the $\delta^{13}C_{org}$ increase. Here, we propose an alternative hypothesis in which the higher $\delta^{13}C_{org}$ values result from the increasing importance of β-carboxylation photosynthetic pathways in marine phytoplankton and C_4 pathways in terrestrial plants in the latter part of the Cenozoic; these pathways produce organic matter with higher $\delta^{13}C$ values than organic matter produced through the C_3 photosynthetic pathway.

For most of the Phanerozoic, marine and terrestrial photosynthetic organisms fixed carbon through a C_3 photosynthetic pathway (Falkowski and Raven,

1997). The long-term depletion of CO_2 associated with greater organic carbon burial since the break-up of Pangea was a key factor that ultimately selected for new photosynthetic pathways in marine and terrestrial ecosystems. Diatoms have β-carboxylation pathways (Morris, 1987; Reinfelder et al., 2000) and are responsible for a disproportionate fraction of carbon export in the modern ocean (Dugdale et al., 1998; Smetacek, 1999). Hence, the rapid radiation of diatoms in the mid-Cenozoic (Fig. 3) must have enriched the ^{13}C composition of marine organic matter. In the late Miocene (6–8 Ma), a major expansion of grasslands throughout most of the world was coupled with a shift in dominance from C_3 to C_4 grasses, producing ^{13}C-enriched terrestrial biomass (Cerling et al., 1997; Still et al., 2003). Consequently, ^{13}C-enriched terrestrial organic matter was ultimately transferred to and sequestered in the oceans (France-Lanord and Derry, 1994; Hodell, 1994) at the same time that ^{13}C-enriched diatoms continued to expand (Fig. 3). The rise of β-carboxylation and C_4 photosynthetic pathways can account for a 1.1‰ decrease in $\delta^{13}C_{carb}$ (based on a 4.4‰ increase in $\delta^{13}C_{org}$ (Hayes et al., 1999) and assuming constant $\delta^{13}C_{input}$, f_{carb}, and f_{org}). Attributing the remaining ~1.4‰ $\delta^{13}C_{carb}$ decrease to weathering of organic-rich shales (as outlined above) requires that an additional ~110 000 Gt of organic carbon was transferred from the continents to the oceans over 15 myr.

4. Summary and conclusions

Our results show that biological and tectonic processes acted in concert to increase the efficiency of organic carbon burial, driving the 190-myr-long depletion of ^{12}C from the ocean–atmosphere system that began in the Jurassic. The resulting long-term increase in $\delta^{13}C$ of the mobile carbon reservoir is apparent in simultaneous increases in $\delta^{13}C_{carb}$ (this study) and $\delta^{13}C_{org}$ (Hayes et al., 1999). This was most likely the result of increases in both f_{org} and $\delta^{13}C_{input}$, which supplied more ^{13}C to and extracted more ^{12}C from the mobile carbon reservoir during the opening phase of the current Wilson cycle.

As Pangea rifted, the enlarging ecospace along newly formed continental margins promoted the diversification and radiation of large-celled eucaryotic phytoplankton. More efficient export production and long-term storage of organic matter along passive continental margins resulted in an f_{org} increase, with corresponding net oxygen production and atmospheric CO_2 drawdown. At the same time that carbon was buried in the circum-Atlantic region, sedimentary carbon was recycled through subduction, delamination, and decarbonation or transfer to orogenic metasediments as the Tethys and Pacific Ocean basins shrank (Selverstone and Gutzler, 1993).

This process demonstrates that continental fragmentation facilitates organic carbon burial, oxidation of Earth's surface reservoirs, and drawdown of atmospheric CO_2, eventually contributing to the switch from the greenhouse climate of the Mesozoic to the icehouse climate of the late Cenozoic. These processes should reverse in the second half of the Wilson cycle as continents reassemble and organic-rich sediments are recycled along the Atlantic margins as the basin closes. This analysis suggests that the geological carbon cycle is strongly influenced by biological processes that control the redox state of the planet and that steady state cannot be approached until a full Wilson cycle is completed.

The long-term depletion of CO_2 associated with greater organic carbon burial was a key factor that selected β-carboxylation and C_4 photosynthetic pathways in marine and terrestrial ecosystems. These new pathways are responsible for the $\delta^{13}C_{org}$ increase in the latter half of the Cenozoic, and contributed to the $\delta^{13}C_{carb}$ decrease that began in the mid-Miocene. The abrupt increase in $\delta^{13}C_{org}$ occurred without a large change in either the atmospheric oxidation state or an injection of ^{12}C from mantle outgassing, and appears to be a unique event in Earth's history. These records show that biological processes play a more significant role in modifying the long-term geological carbon budget than in general has been acknowledged, and have contributed to a global carbon cycle output and planetary redox state that have been out of balance since the Early Jurassic.

Acknowledgements

We thank A.J. Kaufman, M. Pagani, and an anonymous reviewer for their comments. We are grateful to R. Berner, P. Bown, T. Bralower, J.

Browning, L. Burckle, K. Caldiera, C. Cervato, Z. Finkel, J. Hayes, G. Jones, S. Katz, C. Liutkus, A. MacRae, A.J. Milligan, N.J. Shackleton, P. Strother, and K. Wallmann for providing assistance with this project in the form of datafiles, samples, computer model, and/or discussions. This study was supported by NSF OCE 0084032 Biocomplexity: The Evolution and the Radiation of Eucaryotic Phytoplankton Taxa (EREUPT). This research used samples provided by the Ocean Drilling Program (ODP), which is sponsored by the U.S. National Science Foundation (NSF) and participating countries under management of the Joint Oceanographic Institutions (JOI), Inc. Mochras borehole samples were provided by UNOCAL.

Appendix A

$\delta^{13}C$ data are web-archived at http://www.mychronos.chronos.org/~miriamkatz/20040728/.

Appendix B

Age model data are web-archived at http://www.mychronos.chronos.org/~miriamkatz/20040728/.

References

Adatte, T., Stinnesbeck, W., Hubberten, H., Remane, J., Lopez-Oliva, J.G., 2001. Correlation of a Valanginian stable isotopic excursion in northeastern Mexico with the European Tethys. In: Bartoline, C., Buffler, R.T., Cantu-Chapa, A. (Eds.), The Western Gulf of Mexico Basin: Tectonics, Sedimentary Basins, and Petroleum Systems. Amer. Assoc. Petr. Geol.

Alvarez, L.W., Alvarez, W., Asaro, F., Michel, H.V., 1980. Extraterrestrial cause for the Cretaceous–Tertiary extinction. Science 208, 1095–1108.

Arthur, M.A., Dean, W.E., Stow, D.A.V., 1984. Models for the deposition of Mesozoic–Cenozoic fine-grained organic-C rich sediment in the deep sea. In: Stow, D.A.V., Piper, D.J.W. (Eds.), Fine-Grained Sediments: Deep-Water Processes and Facies, Geological Society of London, Special Publication, pp. 527–559.

Bambach, R.K., 1993. Seafood through time: changes in biomass, energetics, and productivity in the marine ecosystem. Paleobiology 19, 372–397.

Bartolini, A., Baumgartner, P.O., Guex, J., 1999. Middle and Late Jurassic radiolarian palaeoecology versus carbon-isotope stratigraphy. Palaeogeogr. Palaeoclimat. Palaeoecol. 145, 43–60.

Berggren, W.A., Kent, D.V., Swisher, C.C., Aubry, M.-P., 1995. A revised Cenozoic geochronology and chronostratigraphy. In: Berggren, W.A., Kent, D.V., Hardenbol, J. (Eds.), Geochronology, Time Scales and Global Stratigraphic Correlations: A Unified Temporal Framework for an Historical Geology. SEPM (Society for Sedimentary Geology), Tulsa, OK, pp. 129–212.

Berner, R.A., 1991. A model for atmospheric CO_2 over Phanerozoic time. Am. J. Sci. 291, 339–376.

Berner, R.A., Kothavala, Z., 2001. GEOCARB III: a revised model of atmospheric CO_2 over Phanerozoic time. Am. J. Sci. 301, 182–204.

Berner, R.A., Beerling, D.J., Dudley, R., Robinson, J.M., Wildman Jr., R.A., 2003. Phanerozoic atmospheric oxygen. Annu. Rev. Earth Planet. Sci. 31, 105–134.

Bown, P.R., Lees, J.A., Young, J.R., 2004. Calcareous nannoplankton diversity and evolution through time. In: Thierstein, H., Young, J.R. (Eds.), Coccolithophores—from Molecular Processes to Global Impact. Springer-Verlag, Berlin, pp. 481–507.

Bralower, T.J., 1999. The record of global change in mid-Cretaceous (Barremian–Albian) secitons from the Sierra Madre, northeast Mexico. J. Foraminiferal Res. 29 (4), 418–437.

Broecker, W.S., Peng, T.-H., 1982. Tracers in the Sea. LDEO of Columbia Univ., Palisades, NY (690 pp.).

Canfield, D.E., Raiswell, R., 1999. The evolution of the sulfur cycle. Am. J. Sci. 299, 697–723.

Cerling, T.E., Harris, J.M., MacFadden, B.J., Leakey, M.G., Quade, J., Eisenmann, V., Ehleringer, J.R., 1997. Global vegetation change through the Miocene/Pliocene boundary. Nature 389, 153–158.

Channell, J.E.T., Erba, E., Lini, A., 1993. Matnetostratigraphic calibration of the Late Valanginian carbon isotope event in peloagic limestones from Northern Italy and Switzerland. Earth Planet. Sci. Lett. 118, 145–166.

Claypool, G.E., Lubeck, C.M., Bayeinger, J.P., Ging, T.G., 1977. Organic geochemistry. In: Scholle, P.A. (Ed.), Geological Studies on the COST No. B-2 Well, U.S. Mid-Atlantic Outer Continental Shelf Area. USGS Circular, pp. 46–59.

Coplen, T.B., 1995. Discontinuance of SMOW and PDB. Nature 375, 285.

Coplen, T.B., Kendall, C., Hopple, J., 1983. Comparison of stable isotope reference samples. Nature 302, 236–238.

D'Hondt, S., Donaghay, P., Zachos, J.C., Luttenberg, D., Lindinger, M., 1998. Organic carbon fluxes and ecological recovery from the Cretaceous-Tertiary mass extinction. Science 282, 276–279.

Derry, L.A., France-Lanord, C., 1996. Neogene Himalayan weathering history and river $^{87}Sr/^{86}Sr$: impact on the marine Sr record. Earth Planet. Sci. Lett. 142, 59–74.

Dickens, G.R., O'Neil, J.R., Rea, D.K., Owen, R.M., 1995. Dissociation of oceanic methane hydrate as a cause of the carbon isotope excursion at the end of the Paleocene. Paleoceanography 10, 965–971.

Dugdale, R., Wilkerson, F., Wilkerson,, 1998. Silicate regulation of new production in the equatorial Pacific upwelling. Nature 391, 270–273.

Erba, E., Channell, J.E.T., Claps, M., Jones, C., Larson, R., Opdyke, B., PremoliSilva, I., Riva, A., Salvini, G., Torricelli, S., 1999.

Integrated stratigraphy of the Cismon Apticore (Southern Alps, Italy): a "reference section" for the Barremian–Aptian interval at low latitudes. J. Foraminiferal Res. 29, 371–391.

Erbacher, J., Thurow, J., 1997. Influence of oceanic anoxic events on the evolution of mid-K radiolaria in the North Atlantic and western Tethys. Mar. Microb. 30, 139–158.

Falkowski, P.G., Raven, J.A., 1997. Aquatic Photosynthesis. Blackwell Science, Malden, MA (375 pp.)

Falkowski, P., Laws, E.A., Barbar, R.T., Murray, J.W., 2003. Phytoplankton and their role in primary, new and export production. In: Fasham, M.J.R. (Ed.), Ocean Biogeochemistry. The Role of the Ocean Carbon Cycle in Global Change. Springer-Verlag, Berlin, pp. 99–121.

Finkel, Z., Katz, M.E., Schofield, O., Wright, J.D., Falkowski, P.G., in press. Climatically-driven evolutionary change in the size of diatoms over the Cenozoic. Proc. Natl. Acad. Sci.

Fischer, A.G. (Ed.), 1984. The two Phanerozoic supercycles. Catastrophes and Earth History. Princeton Univ. Press, Princeton, NJ, pp. 129–150.

Follmi, K.B., Weissert, H., Bisping, M., Funk, H., 1994. Phosphogenesis, carbon-isotope stratigraphy, and carbonate-platform evolution along the Lower Cretaceous northern Tethyan margin. Geol. Soc. Amer. Bull. 106, 729–746.

France-Lanord, C., Derry, L.A., 1994. $\delta^{13}C$ of organic carbon in the Bengal Fan: source evolution and transport of C_3 and C_4 plant carbon to marine sediments. Geochim. Cosmochim. Acta 58, 4809–4814.

Freeman, K.H., Hayes, J.M., 1992. Fractionation of carbon isotopes by phytoplankton and estimates of ancient CO_2 levels. Glob. Biogeochem. Cycles 6, 185–198.

Ghil, M., Allen, M.R., Dettinger, M.D., Ide, K., Kondrashov, D., Mann, M.E., Roberson, A.W., Saunders, A., Tian, Y., Varadi, F., Yiou, P., 2002. Advanced spectral methods for climatic time series. Rev. Geophys. 40.

Gradstein, F.M., Agterberg, F.P., Ogg, J.G., Hardenbol, H., van Veen, P., Thierry, J., Huang, Z., 1995. A Triassic, Jurassic, and Cretaceous time scale. In: Berggren, W.A., Kent, D.V., Hardenbol, J. (Eds.), Geochronology, Time Scales and Global Stratigraphic Correlations: A Unified Temporal Framework for an Historical Geology. SEPM (Society for Sedimentary Geology), Tulsa, OK, pp. 95–126.

Grantham, P.J., Wakefield, L.L., 1988. Variations in the sterane carbon number distributions of marine source rock derived crude oils through geological time. Org. Geochem. 12, 61–73.

Hansen, K.W., Wallmann, K., 2003. Cretaceous and Cenozoic evolution of seawater composition, atmospheric O_2 and CO_2: a model perspective. Am. J. Sci. 303, 94–148.

Haq, B.U., Hardenbol, J., Vail, P.R., 1987. Chronology of fluctuating sea levels since the Triassic (250 million years ago to present). Science 235, 1156–1167.

Harwood, D.M., Nikolaev, V.A., 1995. Cretaceous diatoms: morphology, taxonomy, biostratigraphy. In: Blome, C.D., Whalen, P.M., Reed, K.M. (Eds.), Siliceous Microfossils, Paleontological Society Short Courses in Paleontology. Paleontological Society, Lawrence, KS, pp. 81–106.

Hayes, J.M., Strauss, H., Kaufman, A.J., 1999. The abundance of ^{13}C in marine organic matter and isotopic fractionation in the global biogeochemical cycle of carbon during the past 800 Ma. Chem. Geol. 161, 103–125.

Hedges, J.I., Keil, R.G., 1995. Sedimentary organic matter preservation: an assessment and speculative synthesis. Mar. Chem. 49, 81–115.

Hennig, S., Weissert, H., Bulot, L., 1999. C-isotope stratigraphy, a calibration tool between ammonite- and magnetostratigraphy: the Valanginian–Hauterivian transition. Geol. Carpath. 50, 91–96.

Hodell, D.A., 1994. Magnetostratigraphic, biostratigraphic, and stable isotope stratigraphy of an Upper Miocene drill core from the Sale Briqueterie (northwestern Morocco): a high-resolution chronology for the Messinian stage. Paleoceanography 9, 835–855.

Hodell, D.A., Mueller, P.A., McKenzie, J.A., Mead, G.A., 1989. Strontium isotope stratigraphy and geochemistry of the late Neogene ocean. Earth Planet. Sci. Lett. 92, 165–178.

Howarth, R.J., McArthur, J.M., 1997. Statistics for strontium isotope stratigraphy: a robust LOWESS fit it the marine Sr-isotope curve for 0 to 206 Ma, with look-up table for drivaiton of numeric age. J. Geol. 105, 441–456.

Ivimey-Cook, H.C., 1971. Stratigraphical palaeontology of the Lower Jurassic of the Llandbedr (Mochras Farm) borehole. In: Woodland, A.W. (Ed.), The Llandbedr (Mochras Farm) Borehole. Inst. Geol. Sci, p. 115.

Jenkyns, H.C., Clayton, C.J., 1997. Lower Jurassic epicontinental carbonates and mudstones from England and Wales: chemostratigraphic signals and the early Toarcian anoxic event. Sedimentology 44, 687–706.

Jenkyns, H.C., Gale, A.S., Corfield, R.M., 1994. Carbon- and oxygen-isotope stratigraphy of the English chalk and Italian Scaglia and its palaeoclimatic significance. Geol. Mag. 131 (1), 1–34.

Jenkyns, H.C., Mutterlose, J., Sliter, W.V. (Eds.), 1995. Upper Cretaceous Carbon and Oxygen Isotope Stratigraphy of Deep-Water Sediments from the North-Central Pacific (Site 869, flank of Pikinni-Wodejebato, Marshall Islands), Leg Scientific Res., vol. 143. Ocean Drilling Program, pp. 105–108.

Kent, D.V., Cramer, B.S., Lanci, L., Wang, D., Wright, J.D., Van der Voo, R., 2003. A case for a comet impact trigger for the Paleocene/Eocene thermal maximum and carbon isotope excursion. Earth Planet. Sci. Lett. 211, 13–26.

Kump, L.R., Arthur, M.A., 1999. Interpreting carbon-isotope excursions: carbonates and organic matter. Chem. Geol. 161, 181–198.

Kurtz, A., Kump, L.R., Arthur, M.A., Zachos, J.C., Paytan, A., 2003. Early Cenozoic decoupling of the global carbon and sulfur cycles. Paleoceanography 18 (4), 1090.

Laws, E.A., Bidigare, R., Popp, B.N., 1997. Effect of growth rate and CO_2 concentration on carbon isotopic fractionation by the marine diatom *Phaeodactylum tricornutum*. Limnol. Oceanogr. 42, 1552–1560.

Laws, E.A., Falkowski, P.G., Smith Jr., W.O., McCarthy, J.J., 2000. Temperature effects on export production in the open ocean. Glob. Biogeochem. Cycles 14, 1231–1246.

Leckie, R.M., Bralower, T.J., Cashman, R., 2002. Oceanic anoxic events and plankton evolution: biotic response to tec-

tonic forcing during the mid-Cretaceous. Paleoceanography 17, 1–29.
Lini, A., 1994. Early Cretaceous carbon isotope stratigraphy of the Maiolica Formation, Southern Alps (northern Italy and paleoenvironmental significance). PhD Thesis, Eidg. Techn. Hochsch., Zurich, Switzerland. 259 pp.
Mackenzie, F.T., Pigott, J.D., 1981. Tectonic controls of Phanerozoic sedimentary rock cycling. J. Geol. Soc. (Lond.) 138, 183–196.
Menagatti, A.P., Weissert, H., Brown, R.S., Tyson, R.V., Farrimond, P., Strasser, A., Caron, M., 1998. High-resolution $\delta^{13}C$ stratigraphy through the early Aptian "Livello Selli" of the Alpine Tethys. Paleoceanography 13, 530–545.
Miller, K.G., Fairbanks, R.G., 1985. Oligocene to Miocene carbon isotope cycles and abyssal circulation changes. In: Sundquist, E.T., Broecker, W.S. (Eds.), The Carbon Cycle and Atmospheric CO_2: Natural Variations Archean to Present, Geophys. Monogr. vol. 32. American Geophysical Union, Washington, DC, pp. 469–486.
Miller, K.G., Fairbanks, R.G., Mountain, G.S., 1987. Tertiary oxygen isotope synthesis, sea level history, and continental margin erosion. Paleoceanography 2, 1–19.
Moldowan, J.M., Jacobson, S.R., 2000. Chemical signals for early evolution of major taxa: biosignatures and taxon-specific biomarkers. Int. Geol. Rev. 42, 805–812.
Morettini, E., Santantonio, M., Bartolini, A., Cecca, F., Baumgartner, P.O., Hunziker, J.C., 2002. Carbon isotope stratigraphy and carbonate production during the Early–Middle Jurassic: examples from the Umbria–Marche–Sabina Apennines (central Italy). Palaeogeogr. Palaeoclimat. Palaeoecol. 184, 251–273.
Morris, I., 1987. Paths of carbon assimilation in marine phytoplankton. In: Falkowski, P.G. (Ed.), Primary Productivity in the Sea. Plenum, New York, pp. 139–159.
Padden, M., Weissert, H., de Rafelis, M., 2001. Evidence for Late Jurassic release of methane from gas hydrate. Geology 29, 223–226.
Padden, M., Weissert, H., Funk, H., Schneider, S., Gansner, C., 2002. Late Jurassic lithological evolution and carbon-isotope stratigraphy of the western Tethys. Eclogae Geol. Helv. 95, 333–346.
Paytan, A., Kastner, M., Campbell, D., Thiemens, M.H., 1998. Sulfur isotopic composition of Cenozoic seawater sulfate. Science 282, 1459–1462.
Paytan, F., Martinez-Ruiz, M., Engle, A.I., Wankel, S.D., 2004. Using sulfur isotopes to elucidate the origin of barite associated with high organic matter accumulation events in marine sediments. In: Amend, J.P., Edwards, K.J., Lyons, T.W. (Eds.), Sulfur Biogeochemistry: Past and Present, Special Paper-Geological Society of America vol. 379, pp. 151–160.
Popp, B.N., et al., 1998. Effect of phytoplankton cell geometry on carbon isotopic fractionation. Geochim. Cosmochim. Acta 62, 69–77.
Rau, G.H., Riebesell, U., Wolf-Gladrow, D.A., 1997. Glob. Biogeochem. Cycles 11, 267.
Ravizza, G., 1993. Variations of the $^{187}Os/^{186}Os$ ratio of seawater over the past 28 million years as inferred from metalliferous carbonates. Earth Planet. Sci. Lett. 118, 335–348.
Rea, D.K., Ruff, L.J., 1996. Composition and mass flux of sediment entering the world's subduction zones: implications for global sediment budgets, great earthquakes, and volcanism. Earth Planet. Sci. Lett. 140, 1–12.
Reinfelder, J.R., Kraepeil, A.M.L., Morel, F.M.M., 2000. Unicellular C_4 photosynthesis in a marine diatom. Nature 407, 996–999.
Rohl, H.-J., Schmid-Rohl, A., Oschmann, W., Frimmel, A., Schwark, L., 2001. Posidonia Shale (lower Toarcian) of SW-Germany: an oxygen-depleted ecosystem controlled by sea level and palaeoclimate. Palaeogeogr. Palaeoclimatol. Palaeoecol. 169, 273–299.
Royer, D.L., Berner, R.A., Montanez, I.P., Tabor, N.J., Beerling, D.J., 2004. CO_2 as a primary driver of Phanerozoic climate. GSA Today 14 (3), 4–10.
Scholle, P.A., Arthur, M.A., 1980. Carbon isotope fluctuations in Cretaceous pelagic limestones: potential stratigraphic and petroleum explorations tool. Bull. Am. Assoc. Pet. Geol. 64, 67–87.
Selverstone, J., Gutzler, D.S., 1993. Post-125 Ma carbon storage associated with continent–continent collision. Geology 21, 885–888.
Shackleton, N.J., 1987. Oxygen isotopes, ice volume, and sea level. Quat. Sci. Rev. 6, 183–190.
Shackleton, N.J., Hall, M.A., 1984. Carbon isotope data from Leg 74 sediments. In: Moore, T.C., Rabinowitz, P.D., et al. (Eds.), Inits. Repts. DSDP. U.S. Government Printing Office, Washington, DC, pp. 613–619.
Sheridan, R., Gradstein, F.M., et al., 1983. Init. Repts. DSDP vol. 76. U.S. Govt. Printing Office, Washington, DC. (947 pp.).
Smetacek, V., 1999. Diatoms and the ocean carbon cycle. Protist 150, 25–32.
Smith, A.B., Gale, A.S., Monks, N.E.A., 2001. Sea-level change and rock-record bias in the Cretaceous: a problem for extinction and biodiversity studies. Paleobiology 27 (2), 241–253.
Spencer-Cervato, C., 1999. The Cenozoic deep sea microfossil record: explorations of the DSDP/ODP sample set using the Neptune database. Palaeontol. Electronica 2, 1–270.
Still, C.J., Berry, J.A., Collatz, G.J., DeFries, R.S., 2003. Global distribution of C_3 and C_4 vegetation: carbon cycle implications. Glob. Biogeochem. Cycles 17 (1006).
Stoll, H.M., Schrag, D.P., 2000. High resolution stable isotope records from the Upper Cretaceous rocks of Italy and Spain: glacial episodes in a greenhouse planet? Geol. Soc. Amer. Bull. 112, 308–319.
Stover, L.E., Brinkhuis, H., Damassa, S.P., de Verteuil, L., Helby, R.J., Monteil, E., Partridge, A.D., Powell, A.J., Riding, J.B., Smelror, M., Williams, G.L., 1996. Mesozoic–Tertiary dinoflagellates, acritarchs and prasinophytes. In: Jansonius, J., McGregor, D.C. (Eds.), Palynology: Principles and Applications. Amer. Assoc. Strat. Palynologists Foundation, pp. 641–750.
Strauss, H., 1999. Geological evolution from isotope proxy signals—sulfur. Chem. Geol. 161, 89–101.
Turekian, K.K., Pegram, W.J., 1997. Os isotope record in a Cenozoic deep-sea core: its relation to global tectonics and climate. In: Ruddiman, W.F. (Ed.), Tectonic Uplift and Climate Change. Plenum Press, NY, pp. 383–397.

van de Schootbrugge, B., Föllmi, K.B., Bulot, L.G., Burns, S.J., 2000. Paleoceanographic changes during the early Cretaceous (Valanginian–Hauterivian): evidence from oxygen and carbon stable isotopes. Earth Planet. Sci. Lett. 181, 15–31.

Veizer, J., Ala, K., Azmy, K., Bruckschen, P., Buhl, D., Bruhn, F., Carden, G.A.F., Diener, A., Ebneth, S., Godderis, Y., Jasper, T., Korte, C., Pawellek, F., Podlaha, O.G., Strauss, H., 1999. $^{87}Sr/^{86}Sr$, $\delta^{13}C$ and $\delta^{18}O$ evolution of Phanerozoic seawater. Chem. Geol. 161, 59–88.

Vincent, E., Berger, W.H., 1985. Carbon dioxide and polar cooling in the Miocene: the Monterey Hypothesis. In: Sundquist, E.T., Broecker, W.S. (Eds.), The Carbon Cycle and Atmospheric CO_2: Natural Variations Archean to Present, Geophys. Monogr.AGU, Washington, DC, pp. 455–468.

Wallmann, K., 2001. Controls on the Cretaceous and Cenozoic evolution of seawater composition, atmospheric CO_2 and climate. Geochim. Cosmochim. Acta 65, 3005–3025.

Wallmann, K., 2003. Feedbacks between oceanic redox states and marine productivity; a model perspective focused on benthic phosphorus cycling. Glob. Biogeochem. Cycles 17.

Walsh, J.J., 1988. On the Nature of Continental Shelves. Academic Press, San Diego (520 pp.).

Weissert, H., Lini, A., Follmi, K., Kuhn, O., 1998. Correlation of Early Cretaceous carbon isotope stratigraphy and platform drowning events: a possible link? Palaeogeogr. Palaeoclimatol. Palaeoecol. 137, 189–203.

Wilde, P., Quinby-Hunt, M.S., 1997. Collisions with ice/volatile objects: geological implications—a qualitative treatment. Palaeogeogr. Palaeoclimatol. Palaeoecol. 132, 47–63.

Wilson, J.T., 1966. Did the Atlantic close and then re-open? Nature 211, 676–681.

Woodland, A.W. (Ed.), 1971. The Llanbedr (Mochras Farm) Borehole, Rep. No. 71/18. Inst. Geol. Sci. (115 pp.).

Worsley, T.R., Nance, R.D., Moody, J.B., 1986. Tectonic cycles and the history of the Earth's biogeochemical and paleoceanographic record. Paleoceanography 1 (3), 233–263.

Zachos, J.C., Pagani, M., Sloan, L., Thomas, E., Billups, K., 2001. Trends, rhythms, and aberrations in global climate change 65 Ma to present. Science 292, 686–693.